External reflection Fourier transform infrared spectroscopy: theory and experimental problems [1]

M. Handke *

Department of Materials and Ceramics, University for Mining and Metallurgy (AGH), 30-053 Cracow (Poland)

M. Milosevic and N.J. Harrick

Harrick Scientific Corp., Ossining, NY 10562 (U.S.A.)

(Received 20th April 1990)

Abstract

In the reflection mode of spectroscopic measurements, IR radiation impinges on the surface of a sample and the intensity of the specularly reflected light is recorded. This is an easy to use, non-contact and non-destructive sampling technique suitable for samples with flat and smooth surfaces. The spectra obtained via external reflection depend on a number of factors and differ considerably from standard transmission spectra. These differences are explained and experimental factors that affect the nature of external reflection spectra are discussed.

Keywords: Infrared spectrometry; External reflection

External specular reflection spectroscopy is an IR spectroscopic sampling technique in which the intensity of the radiation reflected from the sample is measured versus the wavelength at the desired angle of incidence and polarization. This technique has been in use from the beginning of the century [1], and it has recently been widely applied to thin films on metal and semiconductor substrates [2–5]. External reflection spectroscopy is ideally suited for samples such as thin films on metal substrates, adsorbed molecules on catalyst surfaces, thin layers of surfactants on semiconductors and adsorbed species on liquid surfaces.

The description of the reflection of light at a single interface between two optical media is given by the Fresnel equations:

$$r_{12}^{\perp} = \frac{n_1 \cos \theta - \sqrt{n_2^2 - n_1^2 \sin^2\theta}}{n_1 \cos \theta + \sqrt{n_2^2 - n_1^2 \sin^2\theta}} \tag{1a}$$

$$r_{12}^{\parallel} = \frac{\dfrac{n_2^2}{n_1}\cos \theta - \sqrt{n_2^2 - n_1^2 \sin^2\theta}}{\dfrac{n_2^2}{n_1}\cos \theta + \sqrt{n_2^2 - n_1^2 \sin^2\theta}} \tag{1b}$$

where r denotes reflectance amplitude coefficient, the symbols $\perp$ and $\parallel$ represent parallel and perpendicular polarization of the light, respectively, θ is the angle incidence and n_1 and n_2 are the complex refractive indices of media 1 and 2 and light is incident from medium 1 (see Fig. 1A).

The most common applications of external reflection are the cases shown schematically in Fig.

1B–D, where three media are separated by two plane parallel interfaces. This are the cases of reflection from a free-standing thin film (Fig. 1B), a film deposited on a flat metal surface (Fig. 1C) and a film on a non-metal partially transparent substrate (Fig. 1D). There are two crucial components in the exact description of light reflection in the above cases. The first deals with the propagation of light through an optical medium and second with the reflection of the light from interfaces between optical media.

Through a homogeneous and isotropic medium, light propagates as a plane wave:

$$\vec{E}(\vec{x}, t) = \vec{E}(0, 0) \exp(i\vec{k}\vec{x} - i\omega t) \tag{2}$$

where the wavenumber k and frequency ω are related by

$$nk_0^2 = k^2, \quad k_0 = \omega/c_0. \tag{3}$$

k_0 is the vacuum wavenumber and k is related to the wavelength λ by

$$k = 2\pi/\lambda \tag{4}$$

for an absorbing medium, the refractive index is a complex number and can be written as

$$n = n_r + ik \tag{5}$$

Equation (2) can now be rewritten as

$$\vec{E}(\vec{x}, t) = \vec{E}(0, 0) \exp\left(in_r\vec{k}_0\vec{x} - i\omega t\right) \exp\left(-k\vec{k}_0\vec{x}\right) \tag{6}$$
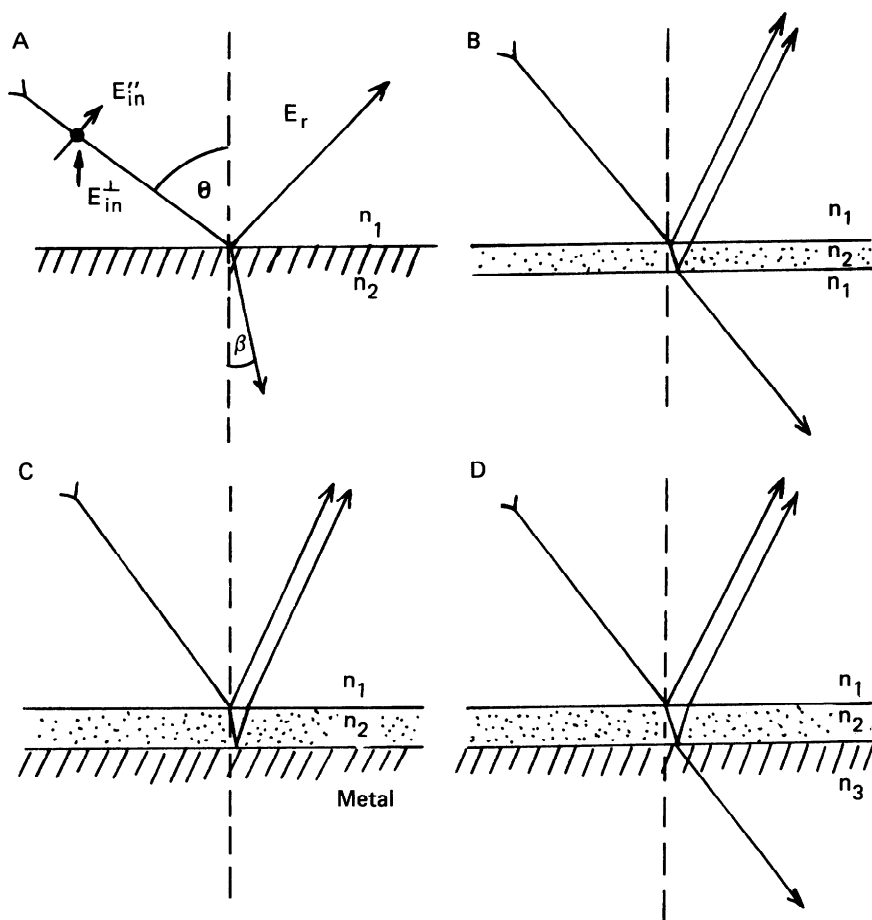

Fig. 1. Optical diagrams for different cases of external reflection: (A) front-surface reflection from semi-infinite samples; (B) reflection from a free-standing film; (C) reflection from a film deposited on a metal substrate; (D) reflection from a film deposited on a non-metal substrate.

As light intensity is proportional to the square of the absolute value of the electric field, Eqn. 6 leads to

$$I(\vec{x}) = I_0 \exp\left(-2k\vec{k}_0\vec{x}\right) \tag{7}$$

The rate of absorption is controlled by the imaginary part of the refractive index, often referred to as the absorption index. Equation 7 is also known as the Lambert–Beer law.

The second important component of reflection of light is described by the Fresnel equations, Eqn. 1. Taking into account the propagation law Eqn. 2 and the Fresnel law for two interfaces; one can find the reflectance amplitude coefficient (ρ^i) for the cases shown in Fig. 1, where i denotes parallel or perpendicular polarization.

$$\rho^i = \frac{r_{12}^i + r_{23}^i \exp\left(2ik_0d\sqrt{n_2^2 - n_1^2 \sin^2\theta}\right)}{1 + r_{12}^i r_{23}^i \exp\left(2ik_0d\sqrt{n_2^2 - n_1^2 \sin^2\theta}\right)} \tag{8}$$

The reflectances of the interfaces are defined as ratios between intensities, not amplitudes. Hence reflectance is the absolute square value of the corresponding amplitude coefficients in Eqn. 8:

$$R^i = |\rho^i|^2 \tag{9}$$

This equation describes external reflection for three media separated by two plane parallel interfaces. For very thin films on light-reflecting substrates the behaviour of light near the reflecting surface requires detailed analysis. In the absence of the sample (i.e., film), the incoming light is superimposed with reflected light, creating a surface wave. It is the resulting electromagnetic field that interacts with molecules of the sample which are placed on the surface. When parallel polarized light is incident on dielectric medium at an incident angle θ, the electric field $\mathbb{E}_{in}$ is perpendicular to the direction of propagation. The incident and reflected waves combine into a surface wave with electric field $\mathbb{E}_s$. The electric field of the surface wave is in the plane of incidence inclined to the normal to the surface at angle $\tan \phi = \cot \theta(1 + |r_{12}''|)/(1 - |r_{12}''|)$. Therefore, for weak reflections the surface field just slightly deviates from the incident field both in direction and magnitude. For a strongly reflecting substrate, the surface field becomes perpendicular

to the interface since then $|r_{12}''| = 1$ and therefore $\phi = 0$. The magnitude of $\mathbb{E}_s$ is given by

$$\mathbb{E}_s^\perp = \sin \theta \mathbb{E}_{in}(1 + |r_{12}|) \tag{10a}$$

$$\mathbb{E}_s^\| = \cos \theta \mathbb{E}_{in}(1 - |r_{12}|) \tag{10b}$$

where $\mathbb{E}_s$ and $\mathbb{E}_{in}$ are the electric fields of the surface and incoming wave, respectively. Note that for highly reflective samples where $|r_{12}''| = 1$ the parallel component of $\mathbb{E}_s$ vanishes at any angle of incidence. For perpendicular polarization both the incident and reflected waves have electric fields parallel to the reflecting surface. Then the magnitude of the surface field is simply $\mathbb{E}_s = \mathbb{E}_{in}(1 - |r_{12}|)$ and is independent of the angle of incidence (except for the dependence implicit in r_{12}). For strongly reflected samples there is no electric field in the surface. Hence molecular dipole moments parallel to the strongly reflecting surface cannot be excited by s-polarized light at any angle of incidence. On the other hand, the component of dipoles perpendicular to the strongly reflecting surface can be excited with p-polarized radiation for large angles of incidence.

The generation of the surface wave in a reflecting surface has important consequences in external reflection spectroscopy. A thin layer of molecules deposited on a strongly reflecting surface (metal) interacts with the surface wave and the strength of absorption of the surface wave by these molecules influences the reflectivity. The surface wave is generated in the illuminated area of the sample. The strength of the absorption is directly proportional to the length of travel of the surface wave along the surface, since it is proportional to the number of molecules that the surface wave encounters as it propagates along the surface. As the angle of incidence changes, the area illuminated by the incident radiation increases as $1/\cos \theta$. It can therefore be said that the absorbed intensity is proportional to the intensity of the surface wave multiplied by the illuminated area of the sample:

$$I_{abs} \sim |\mathbb{E}_s|^2/\cos \theta$$
$$= 4\mathbb{E}_{in}^2 \sin^2\theta/\cos \theta = 4I_0 \sin \theta \tan \theta \tag{11}$$

Therefore, the absorption is proportional to

$$A = \alpha \sin \theta \tan \theta \tag{12}$$

where α is a constant independent of the angle.

The reflected intensity is the difference between the incident and absorbed intensities, and hence the reflectivity is

$$R = 1 - \alpha \sin \theta \tan \theta \qquad (13)$$

The above derivation does not serve to supply the correct theoretical results that should be used in the analysis of the experimental data. The purpose was to develop a clear, intuitive picture to help guide the discussion of the problems and to assist in a qualitative understanding of the processes involved. The result thus obtained is valid only for very weak absorption, owing to the very thin layer.

Spectroscopists using the external reflection technique are mainly interested in light absorption due to vibrational transitions. The aim of this paper is to demonstrate how one can understand the nature of external reflection spectra.

EXPERIMENTAL

Commercially available spectrometers, both dispersive and Fourier transform types, are designed for transmission measurements. Therefore, for reflection measurements, either the spectrometers must be reconstructed or special reflection accessories must be used. There are many commercially available reflection attachments which can be easily installed in the spectrometer. Recently, a new concept for variable-angle reflection measurements was proposed by Harrick Scientific. The optical diagram of this accessory is shown in Fig. 2.
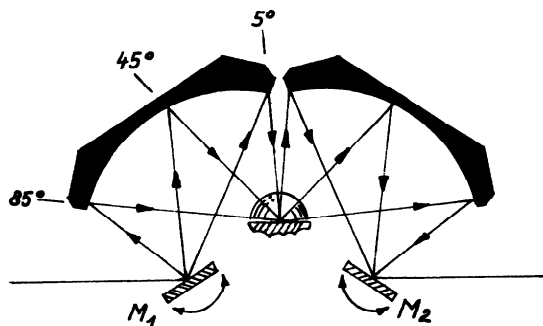

Fig. 2. Optical diagram of the variable-angle reflectance attachment.

Two ellipsoidal mirrors are arranged with a common focal point. The spectrometer beam is focused onto mirror M_1 and can be redirected to various areas of the first illuminating ellipsoid. The ellipsoid has the property to refocus light coming from one focus into the other. The other focus is the sampling point. The sample reflects the light on the second ellipsoid, which redirects the beam to mirror M_2. If mirror M_2 is in the mirror image position to mirror M_1, the light is reflected from M_2 in the same direction as it entered mirror M_1. Therefore, if mirrors M_1 and M_2 are coupled to rotate together and symmetrically, the attachment is automatically aligned at every angle of incidence. This design of the reflection attachment has important advantages: the beam always reflects from the same area of the sample placed stationary in a horizontal orientation; for an imperfectly polished sample the second ellipsoidal mirror collects and transfers to the spectrometer a portion of the light reflected at non-specular angles; and polarization of the light does not change with the angle of incidence and this angle can be continuously changed over a broad range (5–87°).

All the spectra presented were measured with the help of this variable-angle reflection attachment and the polarizer was placed before the reflection attachment.

RESULTS AND DISCUSSION

Spectroscopists using IR external reflection spectroscopic techniques are mainly interested in light absorption due to vibrational transitions. Therefore, external reflection spectra are more useful to them if they resemble transmission spectra, for which large spectral libraries are available. Unfortunately, as mentioned earlier, the external reflection spectra are more dependent on the refractive index than on the absorption coefficient. It is often impossible to obtain a reflection spectrum that fully resembles the corresponding transmission spectrum. In order to obtain analytical information from external reflection spectra, one has to understand all the physical phenomena that affect the nature of such spectra.

The aim of this section is to demonstrate how one can understand the nature of external reflection spectra. For this purpose, the following examples were chosen: external reflection spectra of the air–water interface; external reflection from thin SiO_2 films on aluminium substrates; and external reflection from thin SiO_2 films on silicon substrates. These three cases illustrate important areas of external reflection spectroscopic applications. The air–water interface is an example of two-medium reflection and a gas–liquid interface and the other two are examples of light reflection from three-medium interfaces.

External reflection spectra of air–water interface

In Fig. 3, the optical constants of water (refractive and absorption indices as a function of wavenumber) are shown. These values were calculated by the method proposed by Milosevic [6]. This method is based on the theory of molecular polarizability, from which the dielectric constant can be calculated. The optical constants can then be obtained. This approach is similar to that proposed by Pacansky et al. [7].

In the 4000–400 cm^{-1} range, the refractive index (real part) of water varies between 1.2 and 1.66 while the absorption index (imaginary part of the complex refractive index) varies between 0.0 and 0.4. The reflectivity (Eqn. 1) depends on the complex refractive index. For the air–water interface, the contribution of the real part of n is dominant. This results in the derivative-shaped behaviour of reflectivity within the absorption bands in the reflection spectrum.

In Fig. 4, the specular reflection spectra of water, recorded with the variable-angle reflection attachment, are shown. These spectra were obtained for both perpendicular (s) and parallel (p) polarization for three different angles of incidence: 5° (close to normal), 55° (near the Brewster angle) and 75° (close to the grazing angle). Close to normal incidence, the reflectivities for both s and p polarizations are equal. As the angle of incidence increases, the reflectivity for polarization increases. The reflectivity for p polarization decreases and becomes zero at the Brewster angle, and then increases and becomes unity at 90°. When these spectra are compared with the trans-
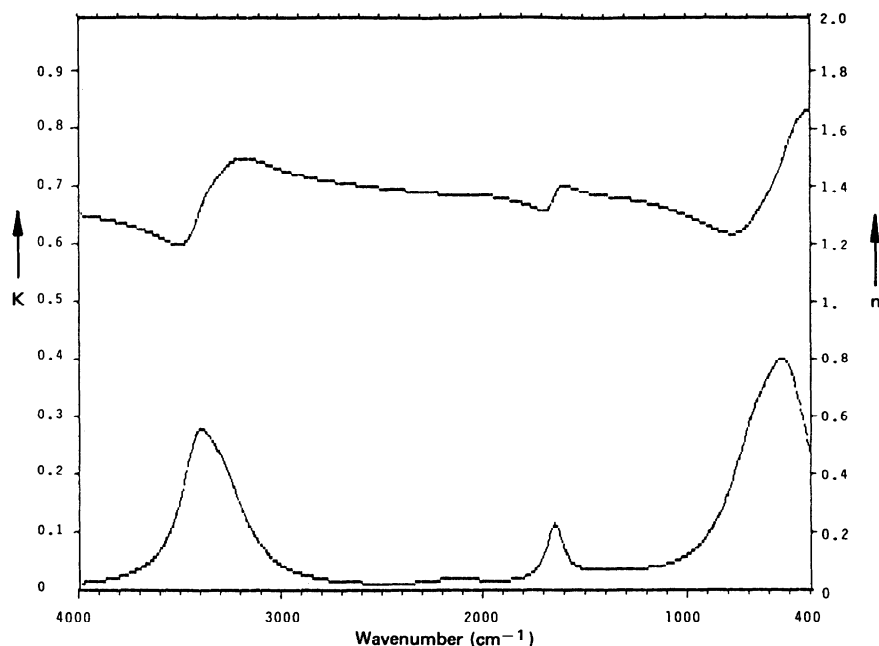

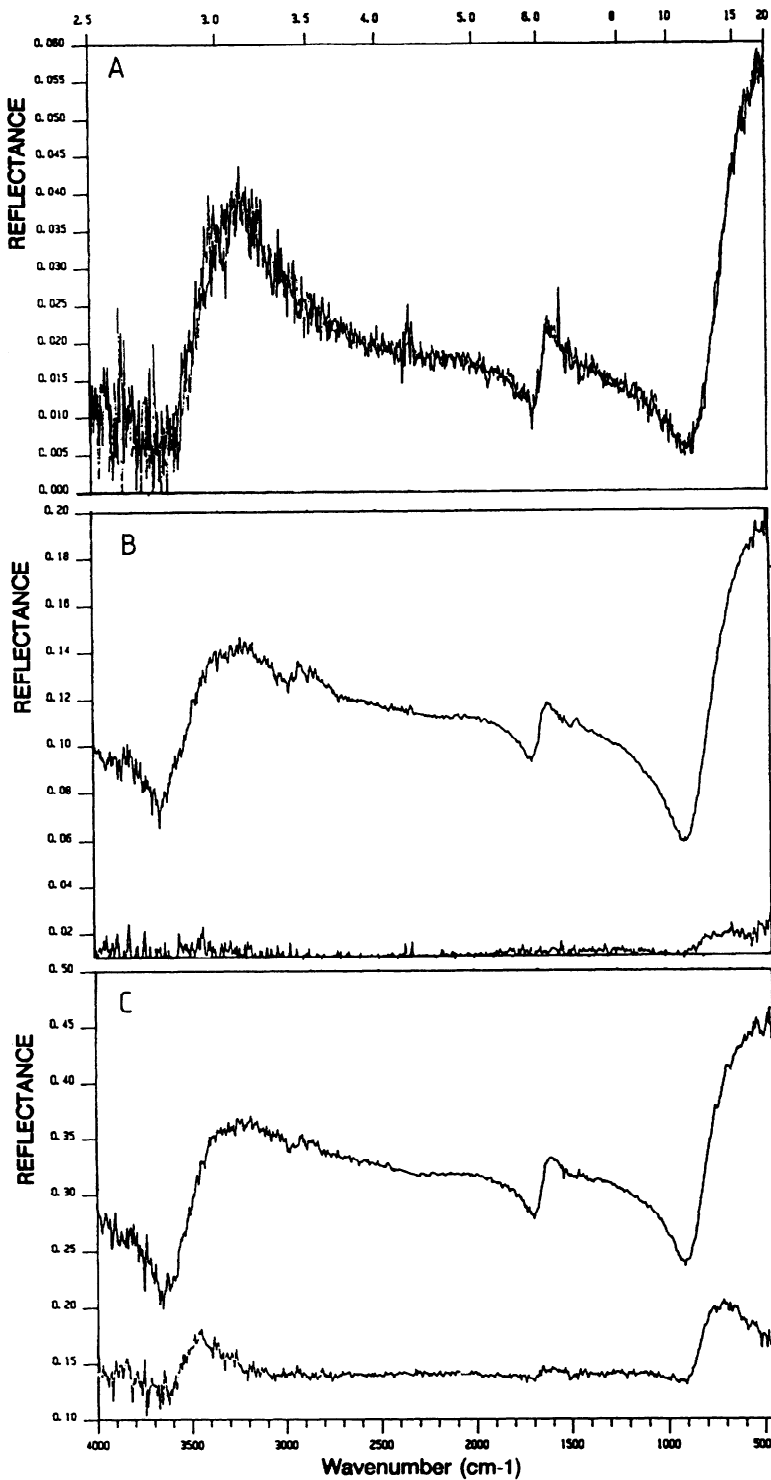Fig. 3. (Top) refractive index (n_r) and (bottom) absorption index (k) of water.

Fig. 4. External reflection for perpendicular (s) and parallel (p) polarization spectra of water recorded at different angles of incidence: (A) 5° (close to normal); (B) 55° (near the Brewster angle); (C) 75° (close to the grazing angle).

mission spectrum of water, the differences in band position and band shape are readily observed. In the IR transmission spectrum, three main bands are observed: OH stretching vibration around 3200 cm^{-1}, H–O–H bending vibration at 1640 cm^{-1} and librational vibration between 600 and 500 cm^{-1}. In these three regions, the real part of the complex refractive index of water changes because of the anomalous dispersion due to the absorption band of water. Because, the reflection is more influenced by the refractive index than the absorption coefficient, the resulting spectrum has a characteristic S shape in the absorption bands.

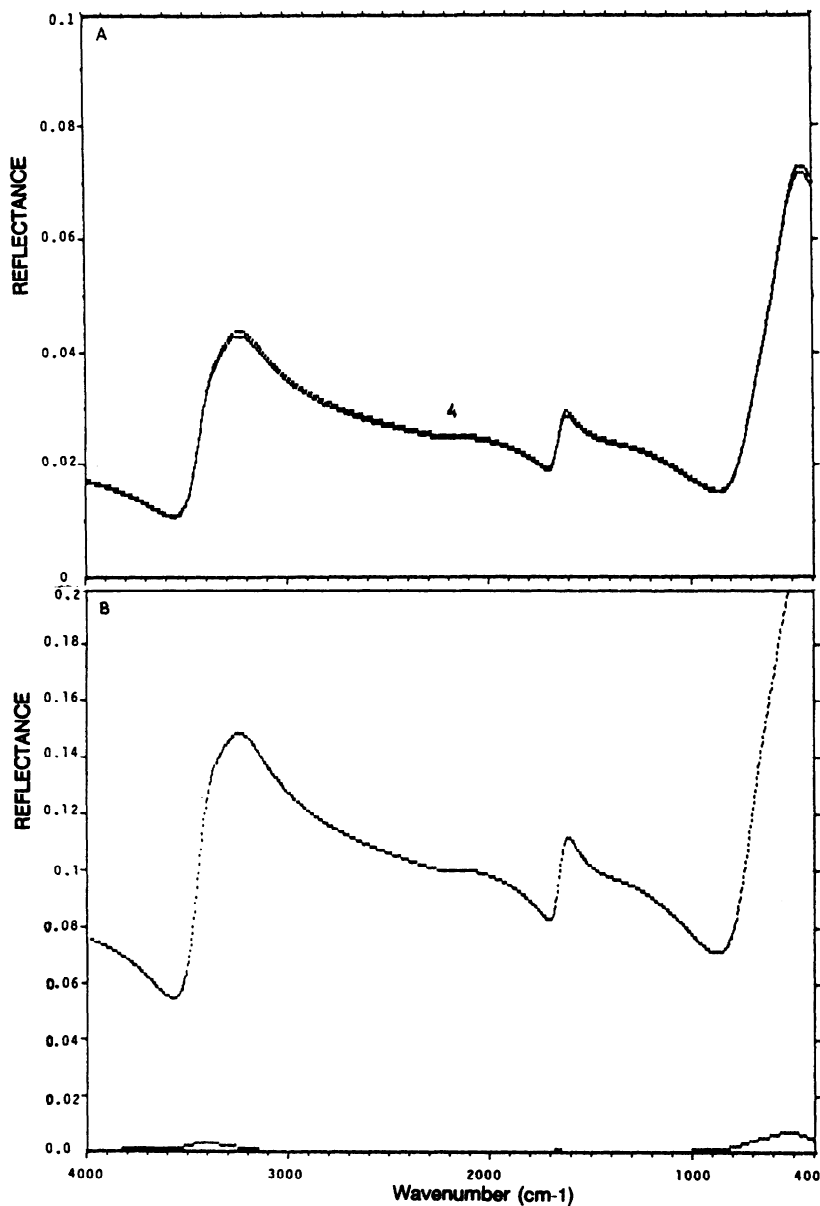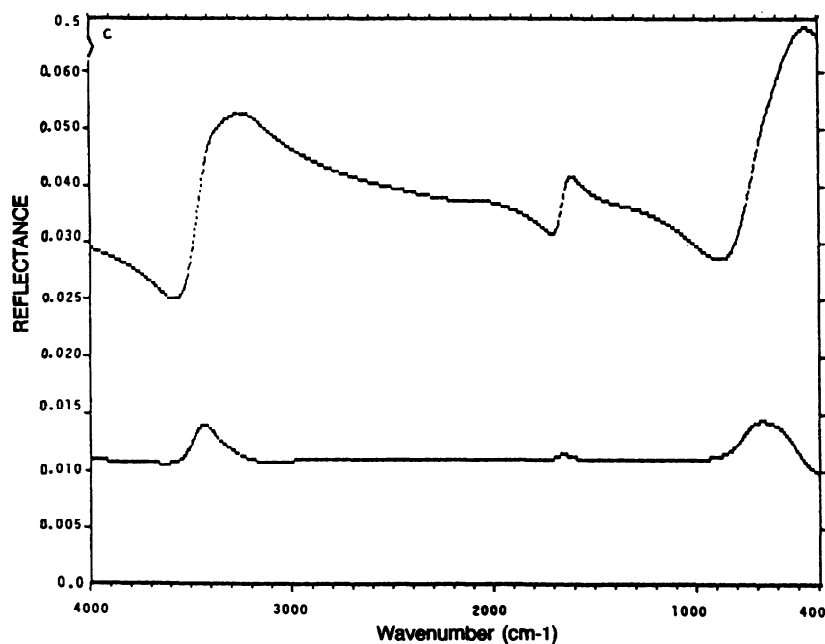The experimental results shown in Fig. 4, are in

Fig. 5.

Fig. 5 (continued). Computer-simulated reflection spectra of water under the measurement conditions as in Fig. 4.

excellent accordance with theory. This can be seen by comparing these spectra with the numerically simulated spectra shown in Fig. 5.

Computer-simulated spectra are, of course, free from noise. Small differences between measured and calculated reflectivity are due to an angular distribution in the incident spectrometer beam. The above experiments show that the external reflection technique can be useful for air–liquid interface studies, where the water is a reflective medium. There are many problems, e.g., insoluble Langmuir–Blodgett monolayers spread at the air–water interface, biophysical monolayer films and biological membranes, where external reflection spectroscopy could provide an important analytical tool.

External reflection spectra of very thin silica film

With measurements of very thin films, some new experimental problems appear. Studies of such films on metal substrates have been widely reported [9,10], but there are still problems with the correct interpretation of these spectra. Examples which demonstrate these problems are the spectra of very thin SiO_2 films on metal and semiconduc-

tor substrates. In Fig. 6, the spectra of a 0.05-μm SiO_2 film on an aluminium mirror are shown. These spectra were recorded with the reflection attachment (see Fig. 2) at 5–85° incidence with perpendicular (Fig. 6a) and parallel (Fig. 6b) polarization.

In Fig. 6a, where the spectra were recorded with s-polarized incident light, the bands due to Si–O vibration are not observed, regardless of the angle of incidence. However, with p-polarized light (Fig. 6b) the bands are clearly seen. With the s-polarized light, despite the angle of incidence, there is an electric field minimum at the interface. This results from the superposition of the incident and the essentially undamped reflected beams. Here the reflected beam is phase shifted by 180° with respect to the incident beam. The incident and reflected light beams superimpose to form a standing wave with electric field strength $\vec{E} = 0$ at the metal surface. The main Si–O absorption region is close to a wavelength of 10 μm. Because the film thickness is 0.05 μm, very little interaction occurs with such a thin film at the metal surface. At one quarter wavelength from the surface, the interaction reaches a maximum. The
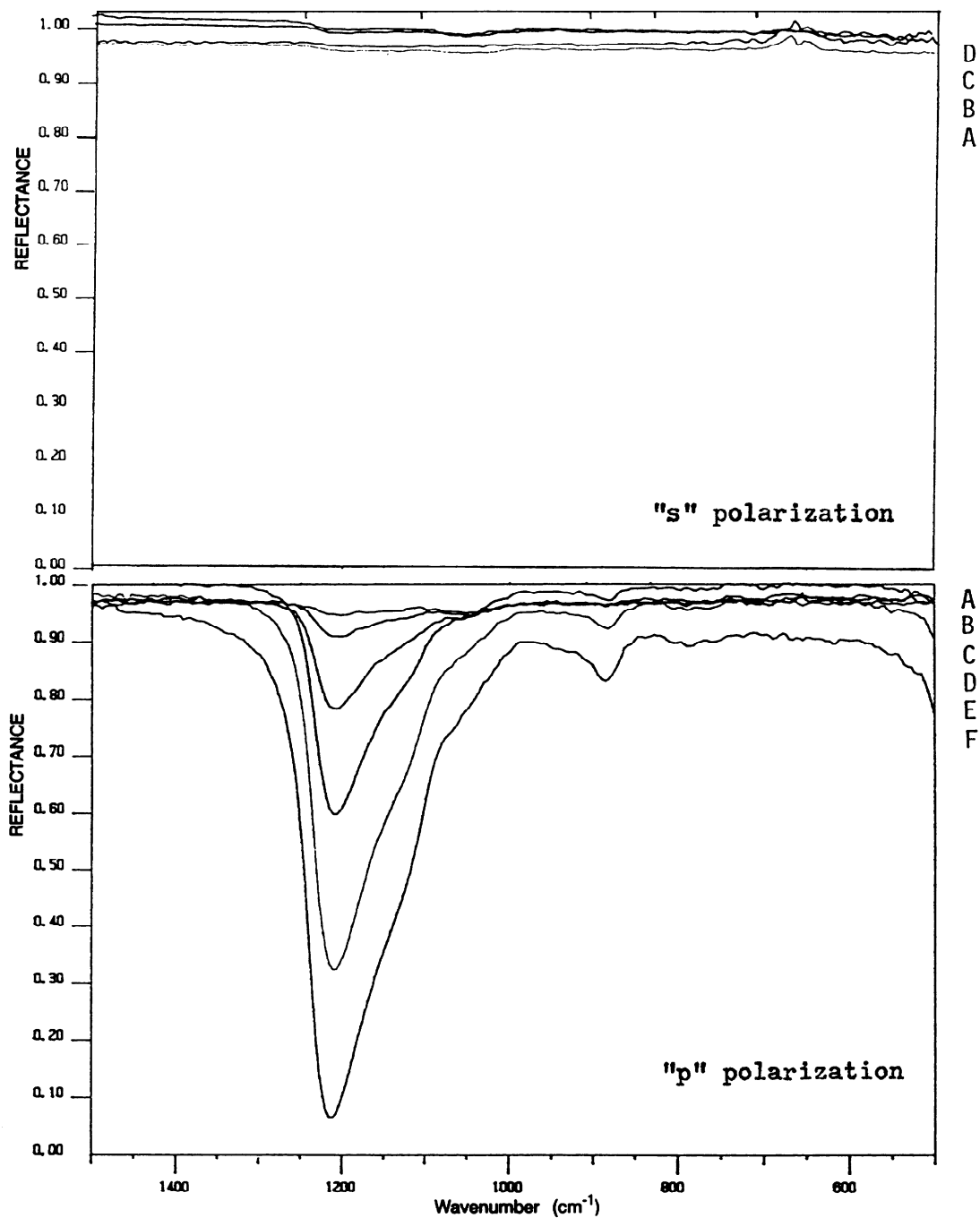
Fig. 6. External reflection spectra of a 0.05-μm film of SiO_2 on aluminium recorded with (a) perpendicular (s) and (b) parallel (p) polarization at different angle of incidence: (A) 5°; (B) 30°; (C) 55°; (D) 70°; (E) 80°; (F) 85°.

interaction becomes zero again at one half wave-length from the metal surface. Therefore, the variation of light absorption with film thickness is not linear. For light with its electric vector polarized parallel to the plane of incident light (p polarization), the electric field vector is parallel to the sample surface only at normal incidence. It varies with the angle of incidence and becomes perpendicular to the sample surface near the grazing angle. In this instance the phase shift of the reflected light varies with the angle of incidence, resulting in large electric field values at the surface for high angles of incidence. Hence, from the standpoint of available excitation energy, the opti-
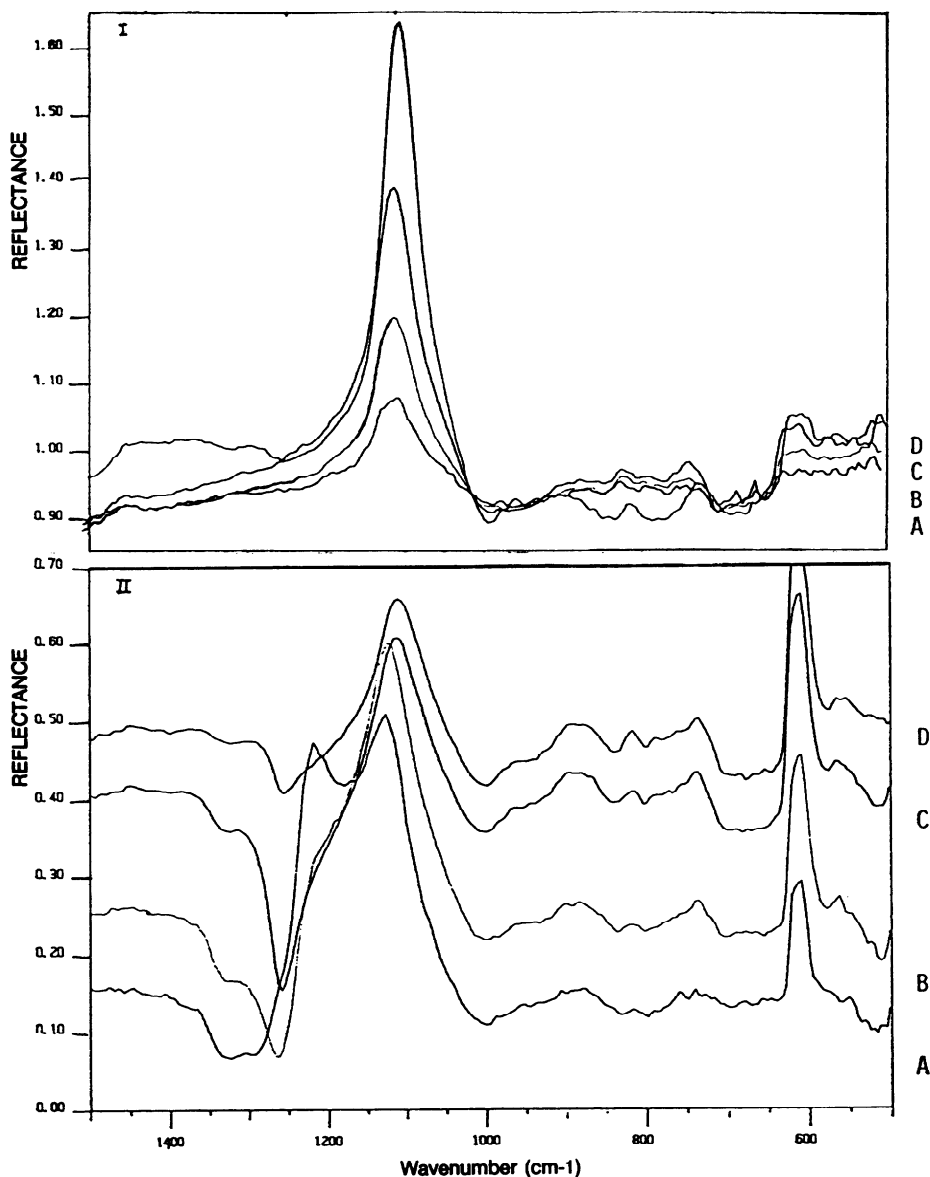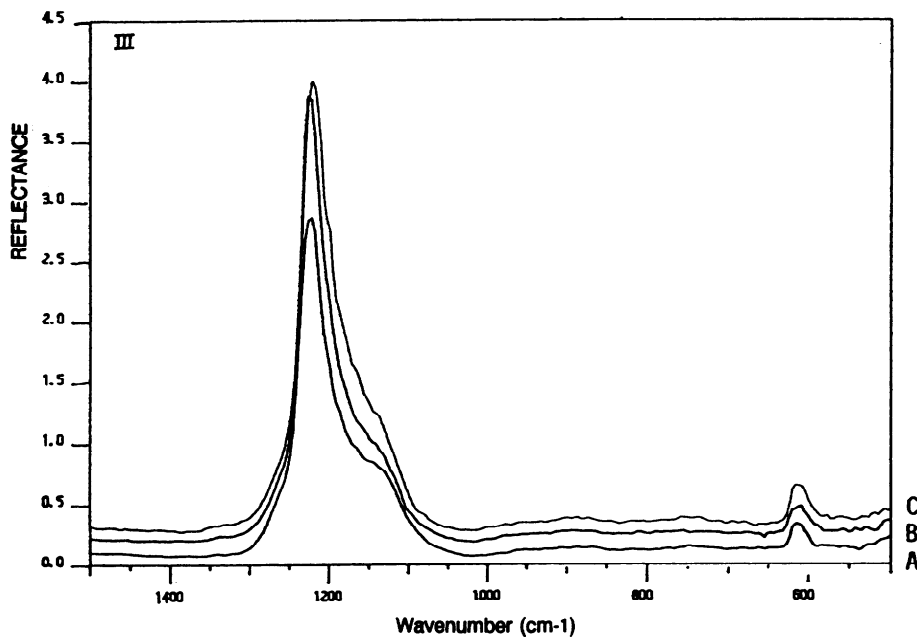
Fig. 7.

Fig. 7 (continued). External reflection spectra of a 0.05-μm film of SiO_2 on silicon: (I) perpendicular (s) polarization at (A) 5°, (B) 55°, (C) 70° and (D) 85° angle of incidence; (II) parallel (p) polarization at (A) 65°, (B) 55°, (C) 30° and (D) 5° angle of incidence; (III) parallel (p) polarization at (A) 70°, (B) 80° and (C) 85° angle of incidence.

mum light interaction occurs for a thin film at large angle and with p-polarized light. This is illustrated in Fig. 6b, where the external reflection spectra of the 0.05-μm thick film of SiO_2 on aluminium are shown. The intensity of the bands here depends strongly on the angle of incidence. At 5° there is virtually no absorption, whereas at 85° the absorption bands reach maximum values. The band maxima in Fig. 6b for the Si-O stretching vibration at 1215 cm^{-1}, the Si-O-Si bridge at 880 cm^{-1} and the O-Si-O bending at 490 cm^{-1} are shifted towards higher wavenumbers in comparison with amorphous SiO_2 transmission spectra (1120, 815 and 460 cm^{-1}, respectively). This is due to the anisotropic nature of the electric field, which selectively excites vibration with transition dipole components perpendicular to the interface. Therefore, in spectra obtained with p-polarized light only LO modes are observed [10].

The external reflection spectra of the same thin film, but on a non-metallic substrate, appear completely different (see Fig. 7). The differences in these spectra are due to the different optical prop-

erties of silicon and aluminium as substrates for the SiO_2 thin film. The spectra in Fig. 7(I) were recorded with s polarization whereas those in Fig. 7(II) and (III) were recorded with p polarization at angles below and above Brewster's angle, respectively. The thickness of the SiO_2 film is the same as on aluminium (500 Å). For s polarization, in contrast to the aluminium substrate, in Fig. 7(I) the band due to Si-O stretching vibration near 1100 cm^{-1} is observed. The intensity of this band decreases with increasing angle of incidence. For p polarization at angles below 60° [Fig. 7(II)], a band at 1100 cm^{-1} is observed in addition to an inverted band at about 1200 cm^{-1}. This inverted band at 60° incidence returns to the normal position and its intensity increases with increasing angle of incidence. It reaches a maximum at the Brewster's angle for silicon [Fig. 7(III)].

These results are in agreement with those recently published by Wong and Yen [11], where similar thicknesses of the SiO_2 films on silicon were studied. They explained the intriguing 1100–1200 cm^{-1} band behaviour in terms of the optical

properties of silicon. However, for a full explanation of this band behaviour, it is necessary to take into account the spectra of SiO_2 films on both aluminium and silicon substrates. The spectrum of SiO_2 on aluminium shows that the vibrational frequencies of Si–O dipoles perpendicular to the metal surface (LO modes) are different from those which are parallel to the metal surface (TO modes). One can observe the TO modes on a non-metal substrate with s-polarized light. For this polarization (despite the angle of incidence), the interaction is possible only with dipoles that have a component parallel to the interface. For p polarization, the electric field vector changes its orientation with angle of incidence. Near normal incidence the electric field is almost parallel to the surface and therefore mainly TO modes are observed in the spectrum [1100 cm^{-1} band in Fig. 7(II)]. As the angle of incidence increases, the contribution of the 1200 cm^{-1} band (LO modes) increases. Other properties, such as changes in the reflection intensities and band inversion (or dispersion), can be explained in terms of the optical properties of silicon as was done by Wong and Yen [11].

For very thin films, TO–LO splitting is common. However, as shown by Yen and Wong [12], it depends on the absorption strength of the film.

Conclusions

The results of external reflection measurements depend strongly on the measurement conditions. Spectra obtained by this technique differ from those obtained by transmission spectroscopy. In order to obtain analytically useful information from external reflection spectra, the physical phenomena responsible for the generation of the spectra should be understood and measurement conditions for a given sample should be carefully chosen.

REFERENCES

1 H. Hagen and W. Rubens, Ann. Phys. (Leipzig), 11 (1903) 873.
2 S.A. Francis and A.H. Ellison, J. Opt. Soc. Am., 49 (1959) 131; R.G. Greenler, J. Chem. Phys., 44 (1966) 310; D.L. Allara, in L.H. Lee (Ed.), Characterization of Metal and Polymer Surfaces, Vol. 2, Academic, New York, 1977.
3 D.L. Allara, A. Baca and C.A. Pryde, Macromolecules, 11 (1978) 1215; H.R. Philipp, J. Appl. Phys., 50 (1979) 1053; Y.S. Yen, J.S. Wong, Mikrochim. Acta, Part I, (1982) 441.
4 G.A. Swallow and G.C. Allen, Oxid. Met., 17 (1982) 141.
5 D. Reinalda and V. Pnec, Surf. Sci., 91 (1980) 1; H.G. Tompkins and R.G. Greenler, Surf. Sci., 28 (1971) 17; M.A. Chesters, F. Parker and R. Raval, Surf. Sci., 165 (1986) 179.
6 M. Milosevic, unpublished data.
7 J. Pacansky, D. England and R. Waltman, Appl. Spectrosc., 40 (1986) 8.
8 R.O. Carter, C.A. Gierczak and R.A. Dickie, Appl. Spectrosc., 40 (1986) 649.
9 J.F. Rabolt, M. Jarick and J.D. Swallen, Appl. Spectrosc., 39 (1985) 269.
10 M. Handke and C. Paluszkiewicz, Infrared Phys., 24 (1984) 121.
11 J.S. Wong and J.S. Yen, Appl. Spectrosc., 42 (1988) 598.
12 Y.S. Yen and Y.S. Wong, paper presented at the 7th International Conference on Fourier Transform Spectroscopy, Fairfax, 1989.